Electronic structure, magnetic, and optical properties of the intermetallic compounds R_2Fe_{17} (R=Pr,Gd)

Yu. V. Knyazev,[1] A. V. Lukoyanov,[1,2] Yu. I. Kuz'min,[1] A. G. Kuchin,[1] and I. A. Nekrasov[1,3]
[1]*Institute of Metal Physics, Russian Academy of Sciences-Ural Division, 620041 Yekaterinburg GSP-170, Russia*
[2]*Ural State Technical University-UPI, 620002 Yekaterinburg, Russia*
[3]*Institute of Electrophysics, Russian Academy of Sciences-Ural Division, 620046 Yekaterinburg, Russia*
(Received 20 October 2005; revised manuscript received 12 January 2006; published 13 March 2006)

In this paper we report comprehensive experimental and theoretical investigation of magnetic and electronic properties of the intermetallic compounds Pr_2Fe_{17} and Gd_2Fe_{17}. Electronic structure of these two systems was probed by optical measurements in the spectral range of 0.22–15 μm. On top of that, charge-carrier parameters (plasma frequency Ω and relaxation frequency γ) and optical conductivity $\sigma(\omega)$ were determined. Self-consistent spin-resolved band-structure calculations within the conventional LSDA+U method were performed. Theoretical interpretation of the experimental $\sigma(\omega)$ dispersions indicates transitions between $3d$ and $4p$ states of Fe ions to be the biggest ones. Qualitatively the line shape of the theoretical optical conductivity coincides well with our experimental data. Calculated by the LSDA+U method magnetic moments per formula unit are found to be in good agreement with observed experimental values of saturation magnetization.

DOI: 10.1103/PhysRevB.73.094410 PACS number(s): 75.50.Ww, 78.20.−e, 71.20.−b

I. INTRODUCTION

During the last two decades Fe-rich intermetallic systems stay under investigation from both experimental and theoretical points of view because of their anomalous magnetic properties. At present the intermetallic compounds with rare-earth elements draw significant interest because of their well-pronounced Invar properties and also as possible new cheap high-energy storing materials for permanent magnets.[1–7] Rare-earth intermetallic compounds R_2Fe_{17} (R is a rare-earth ion) are well known due to the large magnetic moment of Fe ions and yet their comparatively low Curie temperature T_C. Further increase of the T_C of the compounds can be achieved by implantation of interstitial atoms[1,2] or introducing a low content of nonmagnetic impurities substituting Fe atoms.[3–7] In such extended systems, compared to the parent R_2Fe_{17} compounds, upon doping T_C grows more than twice in some cases. This increment of T_C was explained primarily as a result of the lattice expansion with substitution of Fe ions for larger radii ions. According to this concept, Fe-Fe interactions are ferromagnetic or antiferromagnetic for interatomic distance larger or smaller than the critical value 0.25 nm.[8] However, a number of experiments[9–11] showed that in the substitutional $R_2Fe_{17-x}Si_x$ alloys the crystal lattice contracts and the magnetic moment per unit volume decreases, while T_C grows. Later experimental facts are in apparent contradiction with the model.[8] Clearly, a simple approach based on distance-dependent exchange interaction is not sufficient to explain the changes of magnetic properties of these compounds with substitution of Fe for nonmagnetic ions.

Several results of band-structure calculations of the systems from the family are available. For instance, the spin-polarized calculations of electron spectra of $Y_2Fe_{17}N_3$,[12] $Sm_2Fe_{17-x}M_x$ (M=Al,Ga,Si),[13] and $Nd_2Fe_{17-x}M_x$ (M=Si, Ga) (Ref. 14) compounds showed that nonmagnetic impurities modify the shape and width of the spin-up and spin-down densities of states $N(E)$. Jaswal *et al.*[12] suggested to explain the increase of T_C in $Y_2Fe_{17}N_3$ via changes of the density of states at the Fermi level $N(E_F)$ owing to the lattice expansion by means of the Mohn-Wohlfarth static spin-fluctuation model.[15] An analysis of the experimental optical,[7,16,17] low-temperature heat capacity,[7] and photoemission[18] data of some pseudobinary alloys $R_2Fe_{17-x}M_x$ with M=Al,Si revealed a qualitative correlation between the Curie temperature and parameters of electronic structure in the frame of such an approach. Recent experimentally measured optical conductivity of Ce_2Fe_{17} was interpreted in terms of band structure obtained within local-density approximation (LDA).[19]

In accordance with the foregoing systematic study of the electronic structure of R_2Fe_{17} compounds and their modifications with substituted Fe ions, further investigations are of fundamental importance. In this work theoretical calculations of the electronic properties, together with experimental magnetic and optical measurements, were performed. The paper is organized as follows: in Sec. II experimental details and results for Pr_2Fe_{17} and Gd_2Fe_{17} are presented. For instance, Sec. II A is devoted to sample preparation, x-ray-diffraction structural analysis, and magnetic measurements conditions. Section II B provides descriptions of optical experiments. Section III contains results of LSDA+U (Ref. 20) computations of electronic structure and magnetic properties of Pr-Fe and Gd-Fe systems. Structure of experimentally observed optical conductivity curves is anatomized in Sec. IV. At the end we briefly summarize our paper in Sec. V.

II. EXPERIMENT

A. Samples and magnetic measurements

The compounds Pr_2Fe_{17} and Gd_2Fe_{17} were prepared by induction melting in an alumina crucible under argon atmosphere. The ingots were homogenized in the high-purity argon atmosphere at ~1300 K. The purity of the alloys was

TABLE I. Experimental structural, magnetic, and electronic parameters of the intermetallic compounds Pr_2Fe_{17} and Gd_2Fe_{17}: lattice parameters a, c; unit-cell volume at room temperature V; T_C: Curie temperature; M_s: spontaneous magnetization at $T=4.2$ K; relaxation γ and plasma Ω frequencies; N_{eff}: effective concentration of conduction electrons.

Compound	a (Å)	c (Å)	V (Å^3)	T_C (K)	M_s (μ_B/f.u.)	γ (10^{13} s^{-1})	Ω^2 (10^{30} s^{-2})	N_{eff} (10^{22} cm^{-3})
Pr_2Fe_{17}	8.579	12.472	795.0	294	36.1	1.9	21.3	0.67
Gd_2Fe_{17}	8.496	8.341	521.4	466	21.2	1.5	19.5	0.61

checked using standard x-ray diffractometry in Cu $K\alpha$ radiation. The samples were found to be polycrystalline, single-phase, and have rhombohedral structure of the Th_2Zn_{17} type[21] (space group $R\bar{3}m$) for Pr_2Fe_{17} and hexagonal crystal structure of the Th_2Ni_{17} type[22] (space group $P6_3/mmc$) for Gd_2Fe_{17}. The measured lattice parameters a and c are close to those published earlier[21,22] and are shown in Table I. Spherical specimens of 2–3 mm in diameter were used for magnetic measurements. For the following optical studies the specular surface of the samples was prepared by mechanical polishing with diamond pastes.

The Curie points of the compounds were determined from temperature dependencies of ac susceptibility. The ac susceptibility was measured by a differential method in an ac magnetic field of 8 Oe with a frequency of 80 Hz. The saturation magnetizations at $T=4.2$ K were determined from the isothermal magnetization measurements carried out by means of a vibrating sample magnetometer in magnetic fields up to 20 kOe. The magnetic parameters of the compounds are listed in Table I. They are a little different from previously reported data.[23,24] The differences among authors may originate from some deviations of their samples from stoichiometry.

B. Optical measurements

Investigations of optical properties of Pr_2Fe_{17} and Gd_2Fe_{17} were carried out at room temperature by ellipsometric Beattie technique.[25] Spectroscopic ellipsometry is based on the fact that the state of polarization of incident light is changed on reflection. The optical constants—refractive index n and absorption coefficient k—were measured in the spectral range of $\hbar\omega=0.077-5.6$ eV (ω is a cyclic frequency of light) with accuracy of 2–4 %. From n and k, the real $\epsilon_1(\omega)=n^2-k^2$ and imaginary $\epsilon_2(\omega)=2nk$ parts of the complex dielectric function $\epsilon(\omega)$, the optical conductivity $\sigma(\omega)=nk\omega/2\pi$, and the reflectance $R(\omega)=[(n-1)^2+k^2]/[(n+1)^2+k^2]$ were derived. Measurements of reflection spectra followed by Kramers-Kronig analysis were applied to determine the optical parameters in the short-wave range ($\hbar\omega=5.6-8.5$ eV).

The results of optical study (n, k, ϵ_1, ϵ_2, R as functions of ω) for the Pr and Gd compounds are shown in Fig. 1. It is seen that the optical properties of both compounds are rather similar. All directly measured dispersions and further derived quantities are characterized by the broad feature with maximum at the photon energies near 1 eV. As it follows from the line shape of the $\epsilon_2(\omega)$, there is a strong absorption region at energies $\hbar\omega>1$ eV. With increase of the wavelength to infrared range ($\lambda\geqslant 2$ μm) [inset of Fig. 1(a)] the nonmonotonic behavior of n and k is changed by a smooth growth related to the domination of free-electron absorption. Such a character of the frequency dependencies for the optical constants together with negative quantities ϵ_1, as a rule, is typical for the metal-like solids. As one can see from dispersion curves $R(\omega)$, in the low-energy range the reflectance exhibits the high values. The analysis of the energy dependence of ϵ_1 and ϵ_2 in this spectral interval, corresponding to intraband electronic excitations, makes it possible to determine the plasma frequency Ω and the effective relaxation frequency γ of free charge carriers. Within the assumption that light absorption for these energies has Drude character, the parameters $\Omega^2=\omega^2(\epsilon_1^2+\epsilon_2^2)/\epsilon_1$ and $\gamma=\epsilon_2\omega/\epsilon_1$ were computed. In the long-wave region $\lambda>8$ μm, γ and Ω^2 become frequency independent. The values of γ and Ω^2 in this energy interval were used then to estimate the effective concentration of conduction electrons $N_{eff}=\Omega^2 m/4\pi e^2$ (m and e are the mass and the charge of a free electron, respectively). All these parameters obtained from experimental data treatment are presented in Table I.

Optical conductivities $\sigma(\omega)$ for both compounds are displayed in Fig. 2. A monotonic increment of the experimental $\sigma(\omega)$ dispersion observed in the low-energy range is related

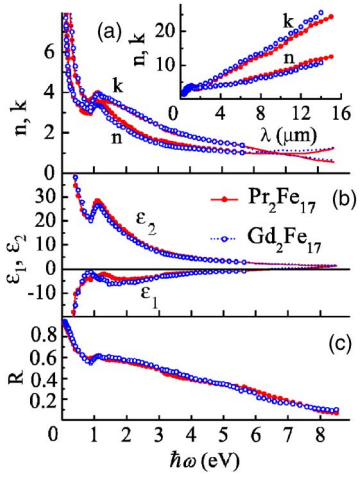

FIG. 1. (Color online) Experimental optical constants n and k (a), dielectric functions ϵ_1 and ϵ_2 (b), and reflectivity spectra R (c) for Pr_2Fe_{17} (full circles and solid line) and Gd_2Fe_{17} (empty circles and dotted line) compounds. Dotted and solid lines above 5.6 eV represent values obtained by Kramers-Kronig transformation from reflection spectra. The inset presents dependences of the optical constants on wavelength for an expanded view in infrared region.

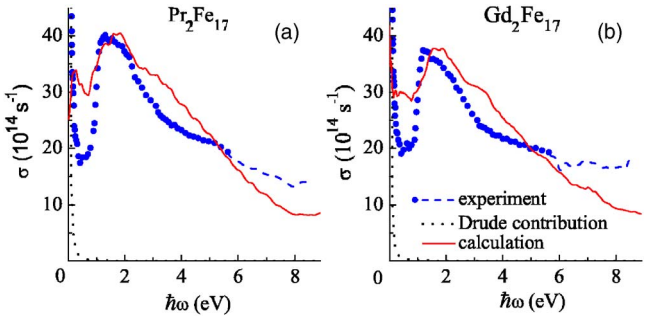

FIG. 2. (Color online) Experimental (dark circles and dashed lines) and calculated (solid lines) dispersion dependencies of optical conductivity for Pr_2Fe_{17} (a) and Gd_2Fe_{17} (b) compounds. Dashed lines represent $\sigma(\omega)$ values obtained by Kramers-Kronig transformation from reflection spectra. Dotted lines correspond to intraband contributions estimated by Drude formula. Calculated values are in arbitrary units.

to the Drude mechanism of electron excitations. For both systems intraband (Drude-like) contributions to the optical conductivity were computed according to the relation $\sigma_{Intra}(\omega)=\Omega^2\gamma/4\pi(\omega^2+\gamma^2)$ and drawn black dotted lines in Fig. 2. Corresponding values of Ω^2 and γ are given in Table I. The magnitude of these contributions falls down sharply with energy and becomes insignificant above 0.5 eV. The values of static conductivity $\sigma_{Intra}(0)$ are estimated to be 0.89×10^{16} s^{-1} for Pr_2Fe_{17} and 1.03×10^{16} s^{-1} for Gd_2Fe_{17} correspondingly. With increase of photon energy the $\sigma(\omega)$ curves show very intense asymmetric stuctures in the near infrared region of spectra at ~1.2 eV. These structures have a pronounced shoulder on the high-energy side and an abrupt low-energy edge. Such behavior is a typical manifestation of the predominance of the interband absorption in this energy interval. The similar shape of the $\sigma(\omega)$ curves was observed early in Y_2Fe_{17}, Ce_2Fe_{17}, and Lu_2Fe_{17} compounds.[17]

III. ELECTRONIC STRUCTURE CALCULATIONS

To calculate electronic structure of the intermetallic compounds under investigation the LSDA+U method[20] within the TB-LMTO-ASA package (tight binding, linear muffin-tin orbitals, atomic-sphere approximation)[26] was applied. Experimentally obtained values of lattice constants for both Pr and Gd systems given in Table I were used in our calculations. Atomic spheres radii were chosen as $R(\mathrm{Pr})=3.91$ a.u. and $R(\mathrm{Fe})=2.62$ a.u. for Pr_2Fe_{17} and $R(\mathrm{Gd})=3.72$ a.u. and $R(\mathrm{Fe})=2.66$ a.u. for Gd_2Fe_{17}. The orbital basis was chosen to be 6*s*, 6*p*, 5*d*, and 4*f* muffin-tin orbitals for Pr or Gd and 4*s*, 4*p*, and 3*d* for Fe sites. The calculations were performed with 32 irreducible **k** points ($6\times6\times6$ spacing) in the first Brillouin zone. Parameters of direct *U* and exchange *J* Coulomb interactions for Gd and Pr ions were calculated by constrained LDA method.[27] For Gd_2Fe_{17} we obtained $U_{Gd}=6.7$ eV and $J_{Gd}=0.7$ eV [similar values were determined previously for elemental Gd (Ref. 20)], and for Pr_2Fe_{17} $U_{Pr}=4.9$ eV and $J_{Pr}=0.6$ eV. Corresponding values of *U* and *J* were applied to Gd and Pr compounds in the frame of the LSDA+U method. Note that, in the present work we do not take into account local Coulomb interaction on Fe ions since constrained LDA gives surprisingly large *U* values.[28] However, for elemental Fe it was shown that an account of Coulomb correlations is important to describe semiquantitatively temperature dependence of magnetization.[29] But on the other hand, such an approach reproduces main structures of LSDA density of states (DOS) with slight modifications of the Fe 3*d* DOS and thus in our case will not strongly affect resulting dispersions of optical conductivity.

TABLE II. Calculated within the LSDA+U method values of local magnetic moments for different sites in Pr_2Fe_{17} and Gd_2Fe_{17} compounds.

Pr_2Fe_{17}		Gd_2Fe_{17}	
Site	$M(\mu_B)$	Site	$M(\mu_B)$
Pr(6*c*)	−2.08	Gd(2*b*)	−7.13
Fe(6*c*)	2.21	Gd(2*d*)	−7.20
Fe(9*d*)	2.23	Fe(4*f*)	2.31
Fe(18*f*)	2.13	Fe(6*g*)	2.10
Fe(18*h*)	2.34	Fe(12*j*)	2.40
		Fe(12*k*)	1.87

Total magnetic moment values per formula units obtained within LSDA+U method ($33.79\mu_B$ for Pr_2Fe_{17} and $21.89\mu_B$ for Gd_2Fe_{17}) are in good agreement with measured experimental data (see Table I). Values of local magnetic moments for different sites for Pr_2Fe_{17} and Gd_2Fe_{17} compounds are listed in Table II. Pr and Gd 4*f* shells are computed to be fully polarized with local moments close to their ionic values while Fe ions have local moment values almost equal to their elemental Fe magnitude. It is remarkable that local moments on rare-earth sites during self-consistent loops become oppositely directed to those on Fe sites. One should also mention that the initial value of local moments on Pr and Gd ions was taken to be zero. Thus *R* and Fe sublattices in our calculations are obtained to be antiferromagnetically ordered.

Calculated in the present work within the LSDA+U method, partial Fe 4*p*,3*d* and rare-earth 5*d*,4*f* DOS for spin-up (↑) and spin-down (↓) projections of local spin moments for Pr_2Fe_{17} and Gd_2Fe_{17} are shown in Figs. 3 and 4. It is seen that the main spectral weight is located in the $E_F\pm5$ eV energy range around the Fermi level. Structures of these DOS are rather similar for both compounds and are qualitatively close to the DOS of ferromagnetic elemental iron in bcc structure.[30] Both these spin-polarized DOSs have a two-peak structure related to the 3*d* states of Fe ions. The Fermi level E_F set to zero lies near the minimum between these two peaks in the spin-down channel and on the upper edge in the spin-up channel. "Spin-up" states of Fe ions are almost completely occupied while "spin-down" states are nearly half filled. The narrow intensive peaks at 3 eV(↓) and 2.7 eV(↑) (Pr_2Fe_{17}) also at −7.3 eV(↓) and 3.5 eV(↑) (Gd_2Fe_{17}) belong to 4*f* states of rare-earth ions. The intensities of Fe 4*s*,4*p* and rare-earth 6*s*, 6*p*, and 5*d* contributions to the DOS are considerably smaller.

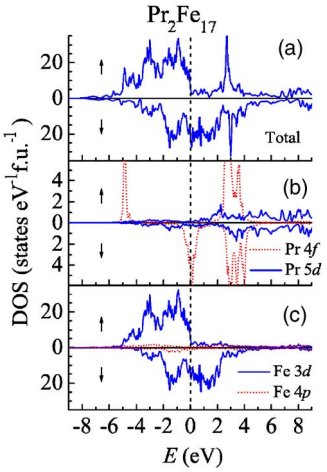

FIG. 3. (Color online) Spin-resolved total (a) and partial 5*d* and 4*f* DOS of rare-earth ion (Pr) (b) and 3*d* and 4*p* densities of states of Fe (c) for Pr_2Fe_{17} compound obtained from the LSDA+U calculation. DOSs were smoothed using adjacent averaging in the interval 0.1 eV. The Fermi level corresponds to zero.

IV. ANALYSIS OF OPTICAL CONDUCTIVITY STRUCTURE

Calculated LSDA+U band structures presented in the preceding section were used to interpret experimental optical conductivity $\sigma(\omega)$ for both intermetallic systems under consideration. In order to calculate theoretical optical conductivity $\sigma_{theor}(\omega)$ and anatomize its ingredients we applied a rather simplified technique similar in spirit to Ref. 31. Namely, we computed the following convolutions representing all possible optical transitions:

$$\sigma_{is}^{ll'}(\omega) = -\frac{1}{\hbar\omega}\int_{E_F}^{E_F+\hbar\omega} N_{il}^{s}(E)N_{il'}^{s}(E-\hbar\omega)dE, \qquad (1)$$

where $N_{il}^{s}(E)$ and $N_{il'}^{s}(E)$ are partial DOSs of the same ion i with the same spin s and orbital quantum numbers l and l' shown in Figs. 3 and 4. The orbital quantum numbers are related by dipole selection rule $l-l'=\pm 1$. Total theoretical

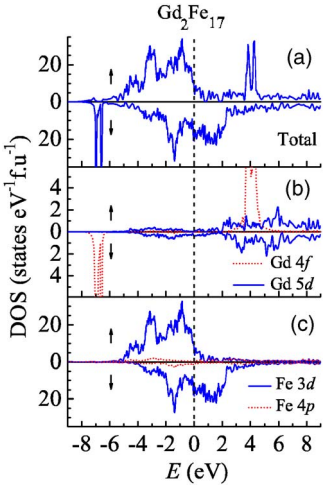

FIG. 4. (Color online) The same as Fig. 3 but for Gd_2Fe_{17}.

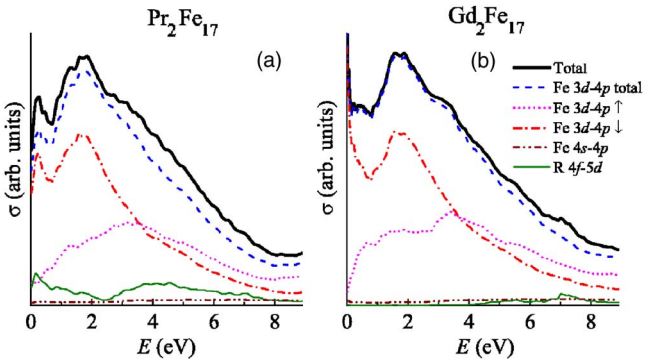

FIG. 5. (Color online) Calculated total (thick solid lines) and partial contributions in optical conductivity for Pr_2Fe_{17} (a) and Gd_2Fe_{17} (b) compounds. Dashed, dotted, and dash-dotted lines show total, spin-up, and spin-down contributions from 3*d*-4*p* transitions in Fe ions, respectively. Dash-dot-dotted lines represent contribution from 4*s*-4*p* transitions in Fe, and thin solid lines correspond to 4*f*-5*d* transitions in rare-earth ions.

optical conductivity is the linear combination of different contributions (1):

$$\sigma_{theor}(\omega) = \sum_{\sigma,i,l-l'=\pm 1} m_i s_{is}^{ll'}(\omega), \qquad (2)$$

where m_i is the degrees of site degeneracy (Wyckoff positions).

Figures 2 and 5 display corresponding $\sigma_{theor}(\omega)$ as solid lines. The overall shape of optical conductivity dispersion curves for both compounds exhibits a broad structure with the peak at ~2 eV. On the whole the theoretical calculations reproduce main features of the experimental $\sigma(\omega)$ curve (Fig. 2): (i) the width of the intense absorption band with distinct maximum, (ii) the sharp threshold in the 0.5–1-eV range, and (iii) the gradual diminution of the high-energy slope.

At the same time there are certain discrepancies. The theoretical peaks are slightly shifted towards the higher energies in contrast to the experimental ones. Also high-energy contributions at 4 eV are slightly overestimated. It may have the following reasons. As was shown by Lichtenstein *et al.*[29] inclusion of local dynamical Coulomb interactions into consideration in elemental Fe will lead to about 30% of correlation bandwidth narrowing. In our case the DOS in the vicinity of the Fermi level consists mostly of the Fe 3*d* states, which are almost identical to those of elemental bcc iron. Roughly one can say that for our intermetallic compounds it can slightly improve comparison with experiment. First of all, a peak at 2 eV could be moved on 0.5–0.6 eV towards lower energies because of correlation narrowing. Second, spectral weight at 4 eV can be transferred to lower energies, and it can give a high-energy tail of theoretical optical conductivity closer to the experimental one. Furthermore, for both systems $\sigma_{theor}(\omega)$ shows a significant interband absorption in the low-energy range ($\hbar\omega < 0.6$ eV), which was not confirmed by the measurements. It is possible that the low-energy absorption, predicted in theory, may be partially disguised in the experimental $\sigma(\omega)$ curves by the strong Drude

rising. The Drude contribution was not taken into consideration in our theoretical model.

Densities of states near the Fermi energy for both compounds mostly consist of the 3*d* states of various crystallographically inequivalent iron ions (see Figs. 3 and 4). A line shape of our LSDA calculated Fe ions DOS is very similar to the known DOS of elemental Fe in the bcc (hcp) phase.[30,32] For the bcc iron it was shown[33] that the optical conductivity determined using the Berglung-Spicer approach[31] agrees rather well with theoretical calculations accounting matrix elements[34] and also with experimental results.[35] This fact enables us to suppose that matrix elements formalism does not play an important role in the case of intermetallic compounds R_2Fe_{17}. In this work we can report our theoretical curves to be in a reasonable qualitative agreement with experimental data.

To analyze the line shape of experimental $\sigma(\omega)$ we provide a detailed description of different contributions to $\sigma_{theor}(\omega)$. As it is seen in Fig. 5 for both systems the biggest contribution to $\sigma_{theor}(\omega)$ comes from 3*d*-4*p* interband optical transitions for Fe ions through the spin-down channel. That gives a high absorption peak at ~2 eV (see dotted curves in Fig. 5). These particular transitions mostly govern low-energy range behavior below 1 eV as well. The second largest contribution is 3*d*-4*p* transitions for Fe ions but in the spin-up channel. In Fig. 5 one can see it as a rather broad structure with maxima at ~4 eV (dot-dashed curves). The contributions from Fe 4*s*-4*p* (Fig. 5, dashed-dot-dot lines) and Pr(Gd) 4*f*-5*d* (Fig. 5, thin solid line) transitions are substantially smaller; and the magnitude of convolutions of rare earths 5*d*-6*p* and 6*s*-6*p* states is negligible.

V. SUMMARY

Comprehensive experimental investigation of structural, magnetic, and optical properties of the intermetallic compounds Pr_2Fe_{17} and Gd_2Fe_{17} was performed during this work. Refined structural parameters are found to be in good agreement with previous data. Measured magnetic properties (i) Curie temperatures T_C=294 K (466 K) and (ii) saturation magnetizations (at T=4.2 K) 36.1 (21.2)μ_B/f.u. for Pr-Fe (Gd-Fe) systems, respectively, also agree well with the literature experimental data. We also report measured optical constants n and k observed at room temperature by ellipsometric Beattie technique in the spectral range of 0.22–15 μm. These experimental data allow us to determine charge-carrier parameters (plasma Ω and relaxation γ frequencies) and optical conductivity $\sigma(\omega)$.

To model magnetic and optical properties of Pr_2Fe_{17} and Gd_2Fe_{17} we did self-consistent spin-resolved calculations within the LSDA+U method. Calculated by LSDA+U method, magnetic moments per formula unit describe well observed experimental values. Furthermore, experimental optical conductivity $\sigma(\omega)$ was interpreted in terms of convolutions between partial densities of states for the same ion, applying dipole selection rule for orbital quantum number. Overall the line shape of experimental and theoretical optical conductivity curves was found to be qualitatively very similar. By anatomizing different contributions to $\sigma_{theor}(\omega)$ it was understood that transitions between 3*d* and 4*p* states of Fe ions give the biggest contribution. The intense peaks in optical conductivity below 1 eV and around 2 eV are predominantly formed by the transitions in the "spin-down" channel, while the second large contribution from "spin-up" channel transitions provides broad feature with the maximum at about 4 eV. The other contributions from rare-earth 4*f*-5*d* and iron 4*s*-4*p* optical transitions are almost negligible.

ACKNOWLEDGMENTS

This work was supported by Grants from the Russian Foundation for Basic Research, Grant Nos. 05-02-17244, 04-02-16096, and 05-02-16301 and in part by programs of the Presidium of the Russian Academy of Sciences (RAS) "Quantum macrophysics" and of the Division of Physical Sciences of the RAS "Strongly correlated electrons in semiconductors, metals, superconductors and magnetic materials." Two of us (I.N., A.L.) acknowledge Dynasty Foundation and International Center for Fundamental Physics in Moscow and Russian Science Support Foundation, Grant of President of Russia MK-02.2118.2005 and interdisciplinary UrO-SO project (I.N.).

[1] J. M. D. Coey and H. Sun, J. Magn. Magn. Mater. **87**, L251 (1990); H. Sun, J. M. D. Coey, Y. Otani, and D. P. F. Hurley, J. Phys.: Condens. Matter **2**, 6465 (1990).
[2] D. B. de Mooij and K. H. J. Buschow, J. Less-Common Met. **142**, 349 (1988).
[3] P. C. M. Gubbens, A. M. Van Der Kraan, T. H. Jacobs, and K. H. J. Buschow, J. Less-Common Met. **159**, 173 (1990).
[4] T. H. Jacobs, K. H. J. Buschow, G. F. Zhou, X. Li, and F. R. de Boer, J. Magn. Magn. Mater. **116**, 220 (1992).
[5] Z. Wang and R. A. Dunlap, J. Phys.: Condens. Matter **5**, 2407 (1993).
[6] B. G. Shen, F. W. Wang, L. S. Kong, and L. Cao, J. Phys.: Condens. Matter **5**, L685 (1993).
[7] A. G. Kuchin *et al.*, Phys. Status Solidi A **155**, 479 (1996).
[8] D. Givord and R. Lemaire, IEEE Trans. Magn. **MAG-10**, 109 (1974).
[9] R. van Mens, J. Magn. Magn. Mater. **61**, 24 (1986).
[10] Z. W. Li, X. Z. Zhou, and A. H. Morrish, Phys. Rev. B **51**, 2891 (1995).
[11] A. G. Kuchin, A. S. Ermolenko, and V. I. Khrabrov, Phys. Met. Metallogr. **86**, 276 (1998).
[12] S. S. Jaswal, W. B. Yelon, G. C. Hadjipanayis, Y. Z. Wang, and D. J. Sellmyer, Phys. Rev. Lett. **67**, 644 (1991).
[13] R. F. Sabirianov and S. S. Jaswal, J. Appl. Phys. **79**, 5942 (1996).
[14] Ming-Zhu Huang and W. Y. Ching, J. Appl. Phys. **79**, 5545 (1996).
[15] P. Mohn and E. P. Wohlfarth, J. Phys. F: Met. Phys. **17**, 2421 (1987).

[16] Yu. V. Knyazev, A. G. Kuchin, and Yu. I. Kuz'min, Phys. Met. Metallogr. **89**, 558 (2000).
[17] Yu. V. Knyazev, A. G. Kuchin, and Yu. I. Kuz'min, J. Alloys Compd. **327**, 34 (2001).
[18] J. P. Woods, B. M. Patterson, A. S. Fernando, S. S. Jaswel, D. Welipitiya, and D. J. Sellmyer, Phys. Rev. B **51**, 1064 (1995).
[19] I. A. Nekrasov, Yu. V. Knyazev, Yu. I. Kuz'min, A. G. Kuchin, and V. I. Anisimov, Phys. Met. Metallogr. **97** (2), 129 (2004).
[20] V. I. Anisimov, F. Aryasetiawan, and A. I. Lichtenstein, J. Phys.: Condens. Matter **9**, 767 (1997).
[21] Q. Johnson, D. H. Wood, and G. S. Smith, Acta Crystallogr., Sect. B: Struct. Crystallogr. Cryst. Chem. **B24**, 274 (1968).
[22] F. Givord and R. Lemaire, J. Less-Common Met. **21**, 463 (1970).
[23] X. C. Kou, F. R. de Boer, R. Grossinger, G. Wiesinger, H. Suzuki, H. Kitazava, T. Takamasu, and G. Kido, J. Magn. Magn. Mater. **177-181**, 1002 (1998).
[24] R. C. Mohanty, C. Zhang, S. A. Shaheen, A. Murugaiah, A. Raman, C. G. Grenier, and R. E. Ferrel, Jr., J. Phys.: Condens. Matter **12**, 9657 (2000).
[25] J. R. Beattie and G. M. Conn, Philos. Mag. **46**, 235 (1955).
[26] O. K. Andersen, Phys. Rev. B **12**, 3060 (1975).
[27] O. Gunnarsson, O. K. Andersen, O. Jepsen, and J. Zaanen, Phys. Rev. B **39**, 1708 (1989).
[28] V. I. Anisimov and O. Gunnarsson, Phys. Rev. B **43**, 7570 (1991).
[29] A. I. Lichtenstein, M. I. Katsnelson, and G. Kotliar, Phys. Rev. Lett. **87**, 067205 (2001).
[30] O. Gunnarsson, Physica B & C **91**, 329 (1977).
[31] C. N. Berglung and W. E. Spicer, Phys. Rev. **136**, A1030 (1964); **136**, A1044 (1964).
[32] S. Wakon and J. Yamashita, J. Phys. Soc. Jpn. **21**, 1712 (1966).
[33] G. A. Bolotin, M. M. Kirillova, and V. M. Maevskii, Phys. Met. Metallogr. **27** (2), 224 (1969).
[34] M. Singh, C. S. Wang, and J. Callaway, Phys. Rev. B **11**, 287 (1975); K. J. Kim, T. C. Leung, B. N. Harmon, and D. W. Linch, J. Phys.: Condens. Matter **6**, 5069 (1994).
[35] V. P. Shirokovskii, M. M. Kirillova, and N. A. Shilkova, JETP Lett. **82**, 784 (1982).